IEEE P802.11
Wireless LANs

Proposed Text for Informative Annex in the IEEE 802.11ay Channel Model Document

Date: 2016-07-25

Author(s):

Name	Affiliation	Address	Phone	email
Minseok Kim	Niigata University	8050 Ikarashi 2-no-cho, Nishi-ku, Niigata, 950-2181 Japan	+81-25-262-7478	mskim@ieee.org
Shigenobu Sasaki	Niigata University		+81-25-262-6737	shinsasaki@ieee.org
Kento Umeki	Niigata University			
Tatsuki Iwata	Niigata University			
Karma Wangchuk	Tokyo Institute of Technology			
Jun-ichi Takada	Tokyo Institute of Technology		+81-3-5734-3288	takada@ide.titech.ac.jp

Abstract

This contribution contains the proposed text on measurement results and simulations related to an outdoor open area access scenario, which will be included to the proposed Informative Annex for the IEEE 802.11ay Channel model document [3]. Main text of this contribution is based on the authors' previous contribution [5].

2. Outdoor Scenario

2.1 Outdoor Open Area Hot Spot Access

2.1.1 Measurement and Simulation Results at 58.5 GHz in Niigata University Campus

2.1.1.1 Measurement Setups

In the measurement, the developed custom channel sounder that employed a commercial product of mm-wave transmitter and receiver (V60TXWG1/V60RXWG1, VubIQ) was used [3]. Using 2 × 2 MIMO configuration full polarimetric wideband channel transfer functions were simultaneously measured. The transmit power of approximately 10 dBm. We exclude the influence of the measurement system from the measured channel responses by full MIMO back-to-back calibration (direct connection between transmitter and receiver antenna ports with a waveguide and an attenuator). The measurement dynamic range is limited to approximately 40 dB. The channel sounding parameters are presented in Table. 1.

The measurement campaign was conducted in an outdoor open square as shown in Fig. 1 where transmitter as an access point (AP) was located at around the center of the area and the channel transfer functions were measured at three positions of the mobile station (MS or STA). STA pos1 and STA pos2 were in LoS condition and STA pos3 was in obstructed-LoS (OLoS) condition. The antenna heights were 3 m for AP and 1.5 m for STA, respectively. The measurement site was surrounded by some large buildings which were located 20 ~ 30 m away from the AP. The distance between AP and STA was approximately 30 m. For acquisition of full polarimetric double-directional channel transfer functions, two orthogonally polarized (ϕ and ϑ) high gain horn antennas were used at both sides of transmitter and receiver, where those antennas were not co-located but direct toward the opposite side (180 degrees) on the same plane. The AP and STA antennas were rotated from 0 to 360 degrees in azimuth, and from −30 to 30 degrees in elevation. Because the half power beam-width (HPBW) are 30 degrees (gain 15 dBi) for STA, and 12 degrees (gain 24 dBi) for AP, respectively, the azimuth and elevation angles at AP and STA were varied in 12 and 30 degree steps, respectively.

Table 2.1: Channel sounding parameters

Carrier Frequency	58.5 GHz
Signal Bandwidth	400 MHz
Sampling Rate	800 MHz
Baseband signal	Unmodulated Multitone
FFT length	512
Tone Spacing	1.563 MHz
Delay Resolution	2.5 ns
Maximum Delay	640 ns
Transmitter Antenna	24dBi Pyramidal Horn
Receiver Antenna	15dBi Pyramidal Horn
Transmitter Antenna Rotation	Az: 0~360 deg., El: 66~114 deg. Step: 12 deg.
Receiver Antenna Rotation	Az: 0~360 deg., El: 60~120 deg. Step: 30 deg.

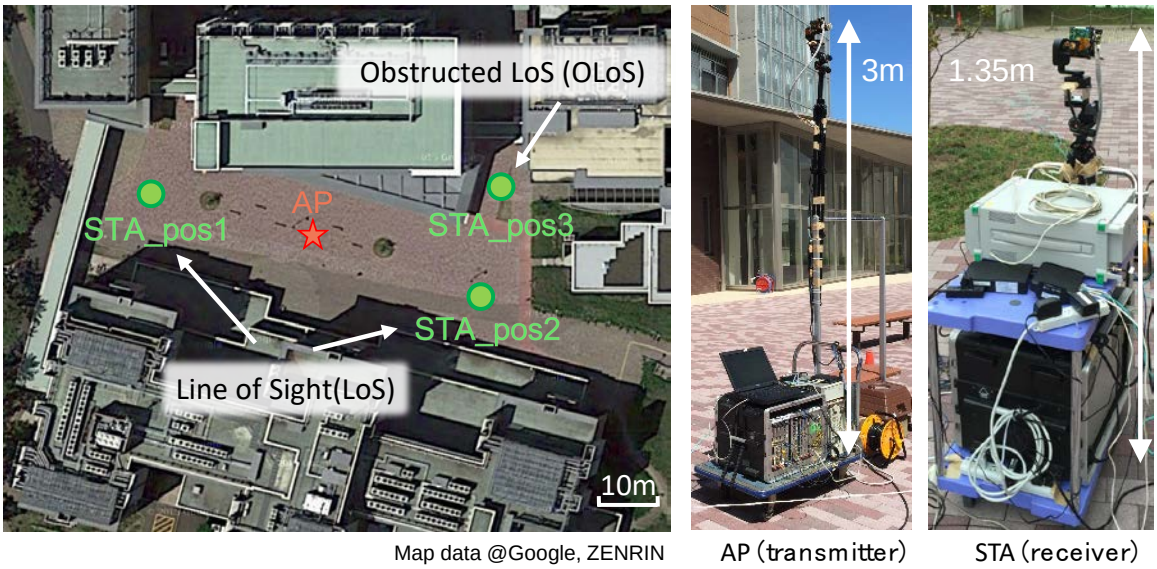

Figure 2.1: Measurement environment

2.1.1.2 Measurement Results

As described in [4], the angle delay power spectrum (ADPS) and angular power spectrum (APS) at both sides of the AP and STA, and the omni-directional power delay profile (PDP) are synthesized from the double-directional ADPS (DDADPS). For precise interpretation of the measurement results, the RT simulation was used applying up to third- and second-order reflections for LoS and OLoS conditions, respectively. The used RT simulation tool employs the image method. The first-order diffraction was further calculated only for OLoS condition based on uniform theory of diffraction (UTD). This simulation calculated the ray parameters of the received power, time delay of arrival, angles of departure (AoD) and arrival (AoA) for each path. For comparison with the measurement results, the simulation based DDADPS was reconstructed from the simulation results by using the radiation patterns of the used antennas, then the APS and PDP were calculated in the same manner as the measurement.

The synthetic ADPSs seen from AP in terms of three different positions of the STA (MS) are shown in Fig. 2.2, where it can be seen that a few significant multi-path clusters are observed besides the LoS path and the dominant paths in the RT results are well matched to those in the measurement results. In addition, comparing the measured and simulated APS of which power are overlapped on the panoramic environment photos and RT simulation results, the propagation mechanism of each cluster has been identified. Some examples are presented in Fig. 2.3.

Table 2 lists the propagation mechanism showing delay, excess loss to the LoS path gain and cross polarization power ratio (XPR) of each cluster, where dominant propagation mechanisms include first- and second-order reflection from the walls of the neighboring buildings, first-order diffraction and scattering by some small objects such as lamppost, tree and weather sheds, and first-order reflection with penetration into glass.

From the channel modeling point of view, it can be concluded as follows. Only a few significant multi-path clusters were observed, and those have relatively small power with the excess loss larger than 20 dB other than the first-order reflection from nearby buildings where the excess loss of the first-order reflection (the second largest cluster in LoS condition) was 11.4, 15.6 and 11.2 dB for STA_pos1, 2, and 3, respectively. It is noted that the distance to the nearby walls was located a bit large from transmitter and receiver. It was also confirmed that when the STA was close to a building wall, the first-order reflected paths could have significantly large power. The first-order reflected paths can be predicted in a deterministic manner, and those should be separately

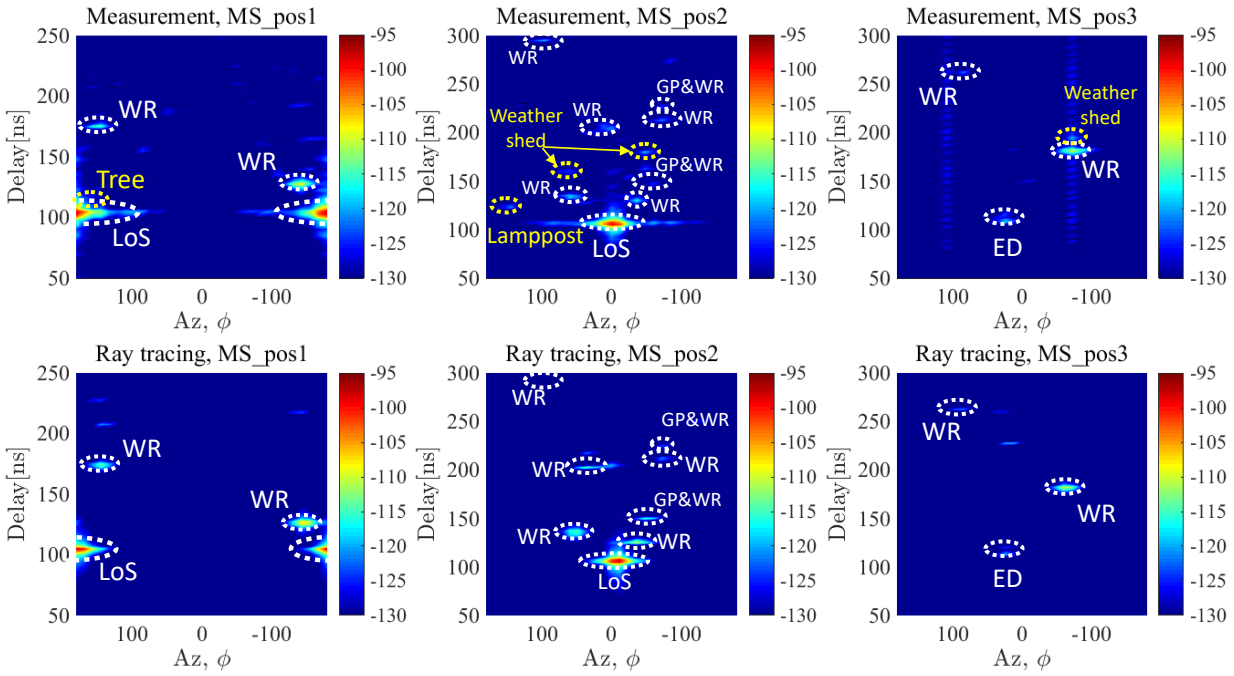

Figure 2.2: Angle delay power spectra (ADPS) observed at the AP in terms of three different positions of STA (LoS, WR, GP and ED are denoted by Line of Sight, Wall Reflection, Glass Penetration and Edge Diffraction)

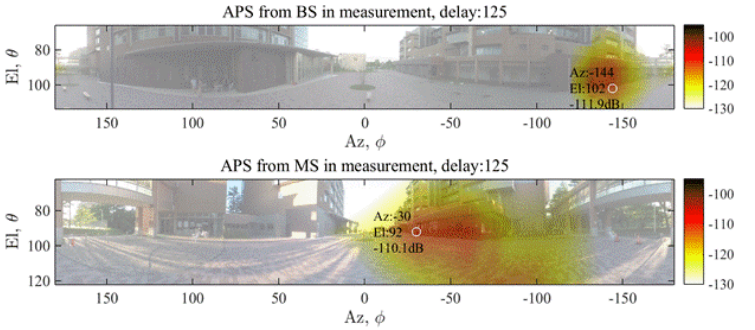

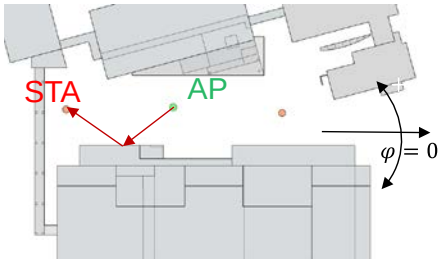

Single bounce wall reflection

(a) STA_Pos1

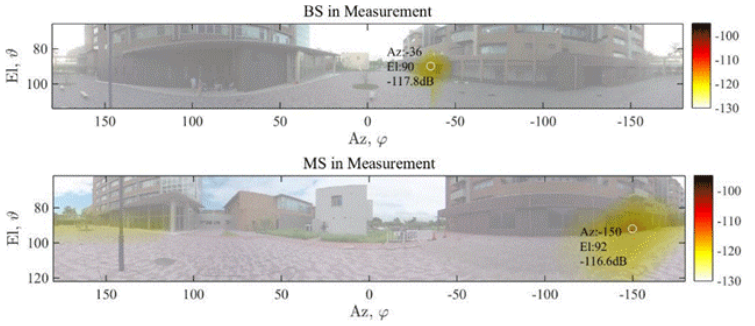

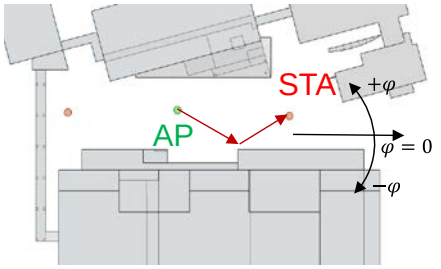

Single bounce wall reflection

(b) STA_Pos2

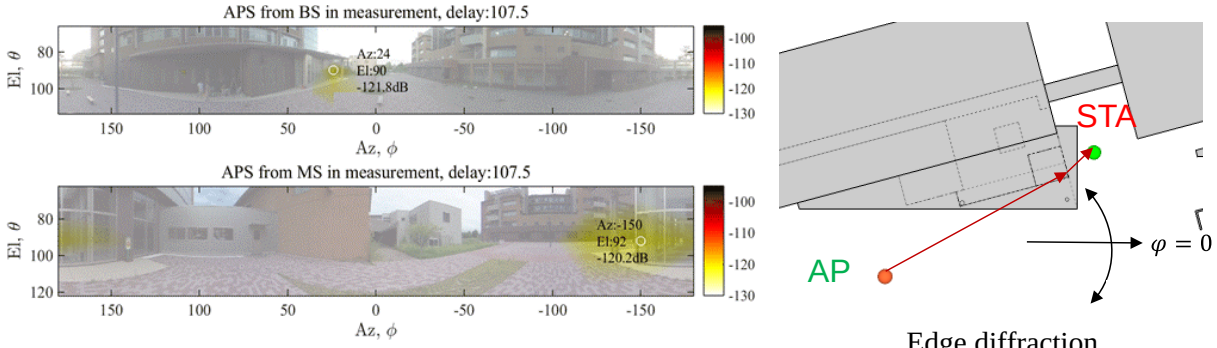

(c) STA_Pos3 Edge diffraction

Figure 2.3: Mechanism identification examples by using APS (left column) and RT output (right column)

2.1.1.3 Channel Modeling

From the above experimental study, a quasi-deterministic (Q-D) modeling approach is considered. That allows natural description of scenario-specific geometric properties, reflection attenuation and scattering, ray blockage and mobility effects [2]. There already exist channel models for open area outdoor hotspot access scenario in [2], where LoS and ground reflection are only considered as D-ray components and determined by the location of Tx and Rx in the surrounding environment assuming that there are no nearby interacting objects in the vicinity of Tx and Rx. The R-ray components such as first- and high-order reflection from far-away static objects and random objects are statistically modeled. Similar to this case as shown in Fig.2.1, if there exists some significant interacting objects such as large buildings, it is reasonable to treat the dominant specular reflection on them as additional Dray components. Based on Q-D model, the statistical channel model parameters of the R-rays were extracted by using RT simulation for more than 300 Rx positions (LoS condition) where the first-order reflected paths from the building walls were eliminated from the estimated ray paths, then the intercluster parameters were calculated simply treating the estimated rays as a cluster. The delay and angle domain parameters are found in [4].

Table 2.2: Identified propagation mechanisms

Propagation Mechanism	STA Position	Delay [ns]	Path Gain [dB]	Excess Loss [dB]	Average Excess Loss [dB]	XPR(TxV)	XPR(TxH)
Single-bounce Reflection	MS_pos1	125	-105.6	10.3	**13.86**	6.39	2.5
	MS_pos2	127.5	-113.5	15.7		8.31	6.98
	MS_pos2	132.5	-113.7	15.9		8.36	8.91
	MS_pos3	180	-108	10.25		13.85	14.36
Double-bounce Reflection	MS_pos1	172.5	-110.4	15.1	**18.49**	10.16	6.41
	MS_pos2	197.5	-117.6	19.8		4.54	3.26
	MS_pos2	210	-116.3	18.5		4.29	6.87
	MS_pos3	260	-117	19.25		3.27	2.56
Diffraction	MS_pos3	107.5	-115	17.25	**17.25**	0.45	10.14
Scattering (Lamppost)	MS_pos2	120	-115.5	17.7	**18.03**	7.13	6.65
Scattering (Tree)	MS_pos1	122.5	-112.6	17.3		13.86	13.94
Scattering (Weather Shed)	MS_pos2	157.5	-116.6	18.8		1.64	8.09
Scattering (Weather Shed)	MS_pos2	177.5	-115.5	17.7		6.57	8.47
Scattering (Weather Shed)	MS_pos3	192.5	-116.2	18.45		6.45	0.8

References:

[1] IEEE Std. 802.11ad-2012, Dec. 2012.
[2] A. Maltsev, et al., Channel Models for IEEE 802.11ay, doc.: IEEE 802.11-15/1150r3, Mar. 2016.
[3] S. Sasaki and M. S. Kim, Proposed Structure of Informative Annex for the IEEE 802.11ay Channel Model Document, doc.: IEEE 802.11-16/0549r0, Apr. 2016.
[4] M. Kim, H. K. Pham and J. Takada, "Development of Low-Cost 60-GHz Millimeter-Wave MIMO Channel Sounding System," Proc. GSMM 2013, Apr. 2013.
[5] M. Kim, et al., "Channel Model for Outdoor Open Area Access Scenarios," IEEE 802.11-16/0342r1, Mar. 2016.